2017

Investigation of the pathological function of PGC1B in the retinal pigment epithelium and its implications for age-related macular degeneration

BOSTON UNIVERSITY

SCHOOL OF MEDICINE

Thesis

INVESTIGATION OF THE PATHOLOGICAL FUNCTION OF PGC1B IN THE RETINAL PIGMENT EPITHELIUM AND ITS IMPLICATIONS FOR AGE-RELATED MACULAR DEGENERATION

by

QUINCY CHARLES

B.S., Stony Brook University, 2013

Submitted in partial fulfillment of the

requirements for the degree of

Master of Science

2017

Approved by

First Reader

Simon Levy, Ph.D.
Associate Professor of Physiology and Biophysics

Second Reader

Magali Saint-Geniez, Ph.D.
Assistant Scientist, Schepens Eye Research Institute
Assistant Professor of Ophthalmology, Harvard Medical School

DEDICATION

I would like to dedicate this work to my parents Circe Charles-Pierre and Jean Leonel Pierre, my late grandmother Marie Leonie Domany, and to the rest of my extended family and friends.

ACKNOWLEDGMENTS

First, I would like to express my sincerest gratitude to Dr. Magali Saint-Geniez for accepting me into her laboratory and giving me the training and guidance needed to successfully complete this thesis project. I would also like to extend my deepest gratitude and appreciation to all of the members of the D'Amore, Arboleda, Kim, Ng, and Saint-Geniez laboratories at the Schepens Eye Research Institute for all the support and assistance they have provided me throughout my time at the institution. I would also like extend my appreciation to Dr. Simon Levy for his guidance and assistance not only for the completion of this thesis, but for the entirety of my time in the Medical Sciences program.

INVESTIGATION OF THE PATHOLOGICAL FUNCTION OF PGC1B IN THE RETINAL PIGMENT EPITHELIUM AND ITS IMPLICATIONS FOR AGE-RELATED MACULAR DEGENERATION

QUINCY CHARLES

ABSTRACT

Age-Related Macular Degeneration (AMD) is a retinal eye disease that is the leading cause of blindness in those over 50 years of age throughout the developed world. Oxidative and metabolic dysfunction of the retinal pigment epithelium (RPE) has been shown to play an important role in AMD. However, the mechanism of dysfunction in the RPE is poorly understood. The peroxisome proliferator-activated receptor-gamma coactivator 1α and β (PGC1A and PGC1B) are coactivators that interact with transcription factors to regulate mitochondria metabolism. In a previous study, it was demonstrated that one of the isoforms, PGC1A, protects RPE cells from oxidative stress through the upregulation of transcription factors that regulate important antioxidant enzymes. There is experimental and clinical evidence that demonstrates that PGC1B may play a deleterious role in the RPE cell. The objective of this study is to characterize the pathological effect of PGC1B on the RPE cell.

PGC1B was overexpressed in the human retinal pigment epithelium cell line (ARPE-19) and expression of the PGC1 isoforms and their main gene targets was evaluated using quantitative polymerase chain reaction (qPCR). Cell death was evaluated under basal and pro-oxidant conditions by quantification of lactate dehydrogenase (LDH) release from the RPE cell. The effect of PGC1B gain of function on the RPE pro-

angiogenic function was evaluated using the choroid explant sprouting assay and by testing the proliferative, migratory, and tube formation potential of RPE-derived conditioned media on the rhesus monkey chorioretinal cell line (RF/6A).

Quantitative PCR analysis showed that overexpression of PGC1B in ARPE-19 cells leads to increased mitochondrial metabolism and decreased antioxidant enzyme expression, causing oxidative stress. After treatment with H_2O_2, PGC1B overexpression caused ARPE-19 cells to become more susceptible to cytotoxicity. The *ex vivo* choroid sprouting assay demonstrated that PGC1B overexpression in RPE is pro-angiogenic. However, cell proliferation as measured by MTT and the cell migration assay provided conflicting results on the pro-angiogenic effect of PGC1B.

Previous research has demonstrated that oxidative stress in the RPE cell plays a role in AMD progression. It has been demonstrated in this study that PGC1B expression leads to increased mitochondrial metabolism and repression of antioxidant enzymes needed to prevent oxidative stress and dysfunction in the RPE cell. While experiments to test the effect of PGC1B on angiogenesis provided conflicting results, a different endothelial cell model may be better suited in demonstrating the pro-angiogenic effect of PGC1B. The hope is that the information provided from this study may be used to further our understanding of AMD and lead to the development of therapeutic targets to combat the effects of AMD.

TABLE OF CONTENTS

LIST OF TABLES

LIST OF FIGURES

LIST OF ABBREVIATIONS

AMD ..... Age-Related Macular Degeneration

AREDS ..... Age-Related Eye Disease Study

BME ..... Basal Membrane Extract

BSA ..... Bovine Serum Albumin

CAT ..... Catalase

cDNA ..... Complementary Deoxyribonucleic Acid

CM ..... Conditioned Media

CMV ..... Cytomegalovirus

CNV ..... Choroidal Neovascularization

DMEM ..... Dulbecco's Modified Eagle's Medium

EGM-2 ..... Endothelial Cell Growth Medium-2

FBS ..... Fetal Bovine Serum

GFP ..... Green Fluorescent Protein

H_2O_2 ..... Hydrogen Peroxide

hfRPE ..... Human Fetal Retinal Pigment Epithelium

LDL ..... Low Density Lipoprotein

MEM ..... Minimum Essential Media

MOI ..... Multiplicity of Infection

MTT ..... 3-(4,5-dimethylthiazol-2-yl)-2,5-Diphenyltetrazolium Bromide

oxLDL ..... Oxidized Low Density Lipoprotein

PBS ..... Phosphate Buffered Saline

PFA ..... Paraformaldehyde

PFU ..... Particle Forming Unit

PGC1A ..... Peroxisome Proliferator-Activated Receptor Gamma Co-Activator 1-Alpha

PGC1B ..... Peroxisome Proliferator-Activated Receptor Gamma Co-Activator 1-Beta

PDGF ..... Platelet-Derived Growth Factor

qPCR ..... Quantitative Polymerase Chain Reaction

RNA ..... Ribonucleic Acid

ROS ..... Reactive Oxygen Species

RPE ..... Retinal Pigment Epithelium

SOD ..... Superoxide Dismutase

SREBP ..... Sterol Regulatory Element-Binding Protein

VEGF ..... Vascular Endothelial Growth Factor

INTRODUCTION

Age-Related Macular Degeneration

Age-Related Macular Degeneration (AMD) is a retinal eye disease that affects the macula which is located in the center of the retina and is essential for high resolution color vision and visual acuity. AMD is the major cause of blindness in individuals over the age of 50 across the developed world.[1] In 2010, it was estimated that 9.1 million people in the United States had early AMD and this number is forecasted to significantly increase to 17.8 million by 2050.[2] Some of the factors that increase the risk of AMD include advanced age,[3] smoking,[4,5] family history,[6] European origin,[7] and genetic mutations.[8-12]

As a person ages, there is an increased deposition of debris, called drusen, between the retinal pigment epithelium (RPE) and the Bruch's membrane of the choroid in the posterior eye. Drusen can be visualized during ophthalmic observation of the fundus of the eye and appears as yellow lesions. The mere presence of small drusen particles (less than 63µm in size) during a funduscopic examination of the eye does not automatically indicate that one has AMD but the presence of larger sized drusen (greater than 63µm) can lead to development of the disease.[13,14]

Ophthalmology researchers and clinicians over the years have developed different systems for classifying the different stages of AMD,[15,16] but to this date no classification system has been universally agreed upon. The Age-Related Eye Disease Study (AREDS) Research Group published a paper that described a classification system for AMD for

clinical application. Early AMD was characterized by the presence of medium sized drusen with no changes in the pigment. Intermediate AMD was characterized by the presence of large drusen (over 125μm in size) and pigment changes. Late AMD was characterized by either choroidal neovascularization (wet AMD) or geographic atrophy (dry AMD).[17] Figure 1 shows images of the different stages of AMD.

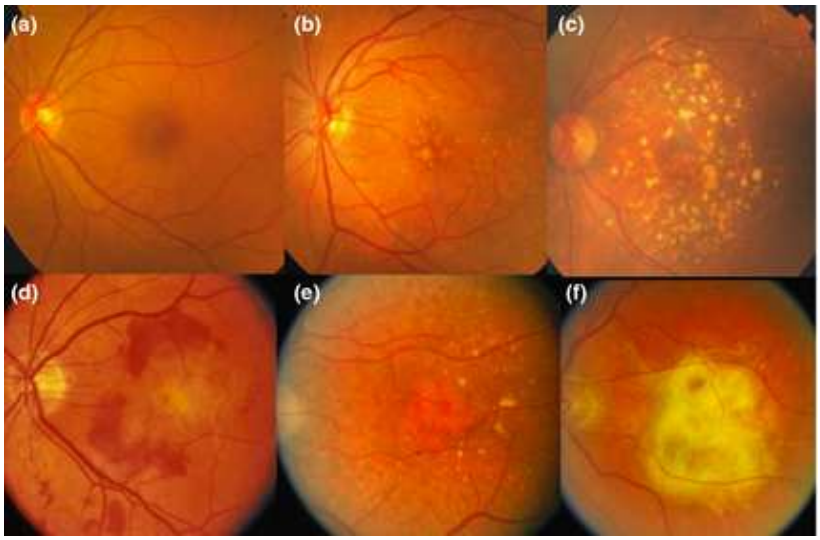

Figure 1: Different Stages of AMD: Panel (a) is the fundus of a normal eye. Panel (b): Patient with early AMD. A few small drusen can be seen. Panel (c): Patient with intermediate AMD with large drusen present. Panel (d): Patient with choroidal neovascularization with hemorrhaging. Panel (e): Patient with geographic atrophy where there has been hypopigmentation of the retinal pigmented epithelium. Panel (f): Scarring as a result of choroidal neovascularization.[18]

Currently, there is no cure for AMD and research has been targeted at developing therapeutics and management strategies to prevent or slow down the progression of the disease. Antioxidant supplementation can be used to reduce the risk of advancing to choroidal neovascularization (CNV) in those with early AMD but is not effective at preventing the onset of the disease.[19,20] Other treatment strategies include dietary and

lifestyle modifications and anti-vascular endothelial growth factor (anti-VEGF) therapy, a very common treatment for CNV.[21-24]

The Role of the Retinal Pigment Epithelium in AMD

The RPE is a monolayer of cells in the outer portion of the retina that is located between the photoreceptor cell layer of the retina and the Bruch's membrane of the choroid. The RPE performs several functions that are vital for a properly functioning retina. Some of the roles of the RPE include light absorption, nutrient and metabolic waste transport, phagocytosis of the photoreceptor outer segments, secretion of growth factors and cytokines such as platelet-derived growth factor (PDGF) and vascular endothelial growth factor (VEGF), visual product cycling, and maintenance of the blood-retina barrier.[25]

As a result of its normal functions, the RPE is exposed to significant oxidative stress on a continuous basis. One source of oxidative stress is the electron transport chain in the mitochondria which is responsible for oxidative phosphorylation to produce ATP for energy. Electrons from the electron transport chain can escape and react with oxygen to form reactive oxygen species (ROS). Uncontrolled accumulation of ROS may lead to oxidative damage and cell death.[26] Phagocytosis of photoreceptor outer segments is another source of oxidative stress to the RPE as the outer segments have already been damaged by photo-oxidation from light absorption.[25] In order to prevent oxidative stress, the RPE relies on a high level of antioxidant enzymes which are regulated in part by the transcription factor NFE2L2 (also known as NRF2).[27]

There is plenty of evidence in the literature that demonstrates that RPE dysfunction due to oxidative stress has been found to cause the progression of AMD.[28,29] Studies in animals have shown that altering oxidative phosphorylation or increasing oxidative stress in the retina or RPE shows some of the same features that are seen in AMD.[30-34] It was also found that in aged eyes or eyes with AMD, there was increased mitochondrial DNA damage due to oxidative stress and a decrease in the expression of certain components of the antioxidant mechanism.[35-37] It also has been found by prior studies that loss of mitochondria integrity, uncontrolled autophagy, and inflammosome activation are part of AMD development and these caused by oxidative stress which shows that RPE dysfunction plays a critical role in the role in the progression of AMD.[38-43]

PGC1 Isoforms

The peroxisome proliferator-activated receptor-gamma coactivator 1α and β (PGC1A and PGC1B) are found in many tissues and organs of the body such as the heart, kidneys, liver, skeletal muscle, and the brain and are critical regulators of mitochondrial metabolism. They interact with DNA binding transcription factors such as estrogen-related receptor alpha (ESRRA), nuclear respiratory factor 1 and 2 (NRF1 and NRF2) in order to activate genes that regulate certain mitochondrial functions which are integral for metabolism.[44,45] Some of the mitochondrial functions that the PGC1 isoforms have the ability to regulate include mitochondrial biogenesis, the electron transport chain, β-oxidation of fatty acids, and the Krebs cycle.[46-48]

PGC1s also play a role in protecting the cell from oxidative damage. As mentioned before, one source responsible for oxidative stress is the electron transport chain in the mitochondria. One way PGC1s protect the cell from oxidative damage is by inducing uncoupling proteins which reduce the inner mitochondrial membrane potential to slow down production of ROS. Another way is by inducing antioxidant enzymes such as superoxide dismutases (SODs) and catalases (CATs) that modify the ROS to be less reactive and damaging to the cell.[49]

The role of PGC1s have been previously studied in other tissues and organs. While PGC1A and PGC1B share certain transcriptional factor targets and functions, there are instances where the roles of PGC1A and PGC1B differ depending on the tissue or organ. It has been shown that PGC1A expression protected neurons from oxidative stress.[49] In type I (slow-twitch) muscle cells, PGC1A has been shown to increase mitochondrial metabolism.[50] In the liver, PGC1A is activated and induces gluconeogenesis in response to starvation.[51] PGC1B is activated upon the intake of dietary fat and coactivates the SREBP transcription factor family to induce lipogenesis.[48] In the retina, PGC1A has been shown to regulate normal and pathological angiogenesis through the induction of VEGF-A expression [52] and protect the retina from damage due to pathologic light exposure.[53] A previous study from our group has shown that during RPE maturation, PGC1A expression is increased while PGC1B expression is repressed in mature RPE. It was found that PGC1A expression in the RPE cell protects it from oxidative damage by inducing the expression of important antioxidant enzymes to reduce

the oxidative stress caused by the normal physiological functions of the RPE cell.[54] However, not much is known about the role that PGC1B plays in the RPE cell.

Preliminary Clinical and Experimental Data

There is clinical and experimental evidence suggesting that PGC1B is involved in AMD progression. Preliminary data from our laboratory has shown that oxidized LDL, which is a component of drusen,[55] triggers RPE death by activating the NRLP3 inflammosome pathway [56] (Figure 2A) and it also induced PGC1B, but not PGC1A, expression (Figure 2B). Clinical data (Courtesy of Dr. Margaret DeAngelis, John A. Moran Eye Center, Salt Lake City, UT) shows that PGC1B expression is specifically increased in the RPE of patients with neovascular AMD compared to control subjects or intermediate (AREDS3) AMD patients (Table 1). Furthermore, there is experimental evidence that overexpression of PGC1B leads to the suppression of anti-angiogenic factors such as thrombospondin-1 (THBS1) and pigment epithelium-derived growth factor (PEDF) (Figure 3).

Table 1: Increased PGC1B Expression Seen In CNV Patients. RNA-sequencing analysis shows that PGC1B (PPARGC1B) expression is induced in patients with choroidal neovascularization (Courtesy of Dr. Margaret DeAngelis, John A. Moran Eye Center, Salt Lake City, UT).

RPE/Choroid Macular Region (n=27 eyes from 27 individuals)						
	Neovascular vs Normal		AREDS3 vs Normal		Neovascular vs AREDS3	
GENE	Fold Change	P value	Fold Change	P value	Fold Change	P value
PPARGC1A	1.120	0.8579	1.503	0.2874	-1.342	0.4910
PPARGC1B	***1.910***	***0.0005***	-1.015	0.9820	***1.937***	***0.0004***

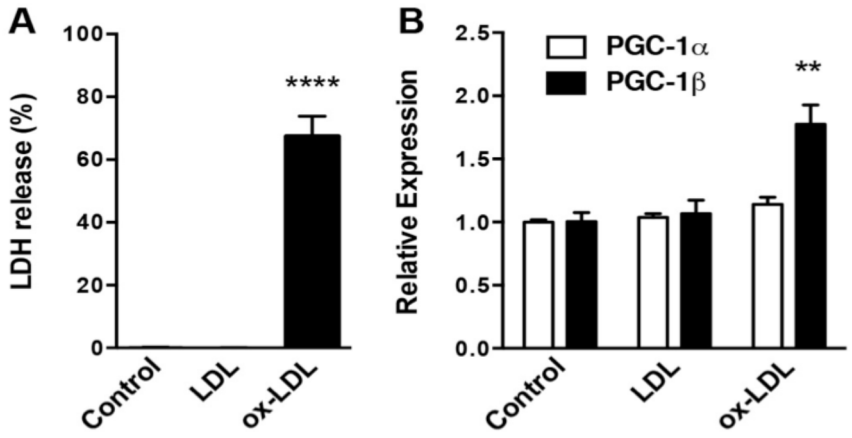

Figure 2: PGC1B expression is induced by oxidized LDL (oxLDL). (A) Measure of LDH release as a marker of cell death in human fetal RPE (hfRPE) after exposure to 500µg/ml of LDL or oxLDL for 48 hours (n=7). Data analyzed using ANOVA. Figure courtesy of Dr. Patricia D'Amore, Schepens Eye Research Institute, Boston, MA. (B) PGC-1α (PGC1A) and PGC-1β (PGC1B) expression levels measured by qPCR in hfRPE after treatment with 500µg/ml of LDL or oxLDL for 24 hours (n=4). Data analyzed using Student's T test. Figure courtesy of Dr. Magali Saint-Geniez, Schepens Eye Research Institute, Boston, MA.

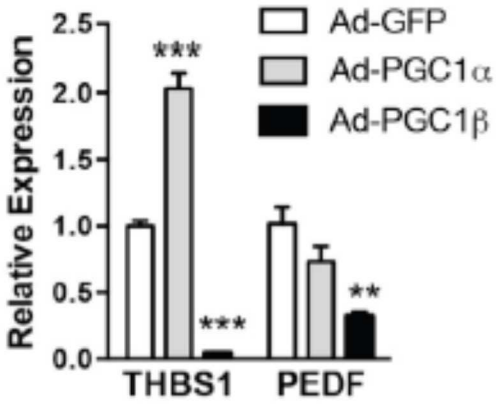

Figure 3: PGC1B overexpression suppresses anti-angiogenic growth factors. qPCR analysis shows that while PGC1A overexpression induces the expression of *THBS1* and *PEDF*, PGC1B overexpression suppressed these anti-angiogenic genes in the RPE (n=3-4). Figure courtesy of Dr. Magali Saint-Geniez, Schepens Eye Research Institute, Boston, MA.

Specific Aims

The PGC1 isoforms are coactivators that are master regulators of mitochondrial metabolism. While they share a number of transcription factor targets and sometimes exert similar effects, prior research has shown that the PGC1 isoforms have divergent effects that is tissue or organ-specific. A previous study has found that RPE cell maturation is associated with PGC1A induction and PGC1B repression. Furthermore, preliminary data from our lab showed that PGC1B is upregulated by cytotoxic doses of oxidized LDL, found to be specifically induced in patients with CNV, and suppresses anti-angiogenic growth factors. Based on these observations, we believe that expression of PGC1B may play a deleterious role in the RPE cell.

Aim 1: To show that PGC1B gain of function has a pro-oxidative effect leading to RPE damage and dysfunction.

Aim 2: To show that PGC1B expression in RPE promotes choroidal neovascularization.

METHODS

Cell Culture

The human retinal pigmented epithelial (ARPE-19, CRL-2302) cell line was obtained from the American Type Culture Collection (ATCC, Manassas, VA). ARPE-19 cells were maintained and expanded in DMEM/F12 media (Lonza, Walkersville, MD) supplemented with 10% Fetal Bovine Serum (FBS, Atlanta Biologicals, Lawrenceville, GA) and 1% penicillin and streptomycin (Lonza). The cells were incubated at 37˚C and 5% CO_2 and split 1:3 when confluent.

The rhesus monkey chorioretinal endothelial (RF/6A) cell line was generously donated by Dr. Budd A. Tucker (Wynn Institute for Vision Research, University of Iowa Carver College of Medicine, Iowa City, IA). The cells were cultured using MEM media (Sigma-Aldrich, Saint Louis, MO) supplemented with 10% FBS (Atlanta Biologicals), 1% penicillin and streptomycin (Lonza), 1% L-glutamine (2mg/L, Lonza), and 1% 1mM sodium pyruvate (Gibco by Life Technologies, Grand Island, NY) and incubated at 37˚C and 5% CO_2. Cells were split 1:3 or 1:4 when confluent.

Evaluation of Adenovirus Transduction Efficiency

ARPE-19 cells were seeded at a density of 20,000 cells/cm^2 and were incubated at 37˚C and 5% CO_2. Twenty-four hours later, the cells were infected with control adenovirus (Ad-GFP, conc: 1.3 x 10^5 pfu/ml), adenovirus containing a mouse PGC1A sequence (Ad-PGC1A, conc: 1.1 x 10^5 pfu/ml), or adenovirus containing a mouse

PGC1B sequence (Ad-PGC1B, conc: 1.5 x 10^5 pfu/ml) at a multiplicity of infection (MOI) of 30, 100, or 300 in serum free media. The Ad-PGC1A and Ad-PGC1B vectors both consist of the GFP gene and the mouse PGC1A and PGC1B genes are located downstream from separate cytomegalovirus (CMV) promoters.[57] Forty-eight hours later, the cells were imaged using an EVOS fluorescent microscope (Life Technologies, Carlsbad, CA) and the percentage of transduced GFP-positive cells was evaluated.

RNA Extraction and Quantitative PCR (qPCR)

Total RNA was isolated from cells using RNA-Bee (Tel-Test Inc., Friendswood, Texas, USA) according to the manufacturer's directions. RNA pellets were reconstituted using Tris-EDTA buffer solution (Ambion, AM9849). RNA concentration and purity were measured using the NanoDrop 2000 spectrophotometer (Thermo Fisher Scientific, Wilmington, DE). One microgram of RNA was reverse-transcribed into complementary DNA (cDNA) using the iScript cDNA synthesis kit (Bio-Rad Laboratories, Hercules, CA) according to manufacturer's directions. Quantitative polymerase chain reaction (qPCR) was performed using the Lightcycler480 system with the Fast Universal SYBR Green Master Mix (Roche Life Sciences, Indianapolis, IN) to analyze the expression of antioxidant and transcription factor genes that are regulated by the PGC1 isoforms. Table 2 contains a list of the primers used and their sequences. Relative gene expression was calculated using the $2^{-\Delta\Delta Ct}$ method and normalized using the housekeeping genes *B2M*, *HPRT1*, and *PPIA*.

Table 2: Primer Sequences for qPCR

Gene Abbreviation	Gene Name	Primer Sequence	
eGFP	Enhanced Green Fluorescent Protein	Forward (5'-3')	AAGCAGCACGACTTCTTCAAGTC
		Reverse (5'-3')	TCGCCCTCGAACTTCACCTC
qhB2M	Human Beta-2-microglobin	Forward (5'-3')	AAGATTCAGGTTTACTCACGTC
		Reverse (5'-3')	TGATGCTGCTTACATGTCTCG
qhCAT	Human Catalase	Forward (5'-3')	ACTTTGAGGTCACACATGACATT
		Reverse (5'-3')	CTGAACCCGATTCTCCAGCA
qhESRRA	Human Estrogen-related receptor alpha	Forward (5'-3')	TATGGTGTGGCATCCTGTG
		Reverse (5'-3')	GTCTCCGCTTGGTGATCTC
qhFOXO3	Human Forkhead box O3	Forward (5'-3')	CTTCAAGGATAAGGGCGACA
		Reverse (5'-3')	AGTTCCCTCATTCTGGACCC
qhHMOX1	Human Heme oxygenase (decycling) 1	Forward (5'-3')	GCCAGCAACAAAGTGCAAG
		Reverse (5'-3')	GAGTGTAAGGACCCATCGGA
qhHPRT1	Human Hypoxanthine Guanine Phosphoribosyltransferase 1	Forward (5'-3')	CCTGGCGTCGTGATTAGTGAT
		Reverse (5'-3')	AGACGTTCAGTCCTGTCCATAA
qhNFE2L2	Human Nuclear factor, erythroid 2-like 2	Forward (5'-3')	TCCAGTCAGAAACCAGTGGAT
		Reverse (5'-3')	GAATGTCTGCGCCAAAAGCTG
qhNRF1	Human Nuclear respiratory factor 1	Forward (5'-3')	GCTGATGAAGACTCGCCTTCT
		Reverse (5'-3')	TACATGAGGCCGTTTCCGTTT
qhPGC1A	Human Peroxisome proliferator-activated receptor gamma, coactivator 1 alpha	Forward (5'-3')	GTCACCACCCAAATCCTTAT
		Reverse (5'-3')	ATCTACTGCCTGGAGACCTT
qhPGC1B	Human Peroxisome proliferator-activated receptor gamma, coactivator 1 beta	Forward (5'-3')	CCACATCCTACCCAACATCAAG
		Reverse (5'-3')	CACAAGGCCGTTGACTTTTAGA
qhPPARA	Human Peroxisome proliferator-activated receptor alpha	Forward (5'-3')	ATCGAATGTAGAATCTGCGGG
		Reverse (5'-3')	TCGCACTTGTCATACACCAG
qhPPIA	Human Peptidylprolyl isomerase A (cyclophilin A)	Forward (5'-3')	CAGACAAGGTCCCAAAGACAG
		Reverse (5'-3')	TTGCCATCCAACCACTCAGTC
qhSOD2	Human Superoxide dismutase 2, mitochondrial	Forward (5'-3')	CAGACCTGCCTTACGACTATGG
		Reverse (5'-3')	CGTTCAGGTTGTTCACGTAGG
qhTXN2	Human Thioredoxin 2	Forward (5'-3')	TGATGACCACACAGACCTCG
		Reverse (5'-3')	ATCCTTGATGCCCACAAACT

Table 2 Continued. Primer sequences for qPCR

Gene Abbreviation	Gene Name	Primer Sequence	
qmB2M	Mouse Beta-2-microglobin	Forward (5'-3')	TTCTGGTGCTTGTCTCACTGA
		Reverse (5'-3')	CAGTATGTTCGGCTTCCCATTC
qmPGC-1α	Mouse Peroxisome proliferator-activated receptor gamma, coactivator 1 alpha	Forward (5'-3')	AGCCGTGACCACTGACAACGAG
		Reverse (5'-3')	GCTGCATGGTTCTGAGTGCTAAG
qmPGC-1β	Mouse Peroxisome proliferator-activated receptor gamma, coactivator 1 beta	Forward (5'-3')	CCCAGCGTCTGACGTGGACGAGC
		Reverse (5'-3')	CCTTCAGAGCGTCAGAGCTTGCTG
qmPPIA	Mouse Peptidylprolyl isomerase A (cyclophilin A)	Forward (5'-3')	GAGCTGTTTGCAGACAAAGTTC
		Reverse (5'-3')	CCCTGGCACATGAATCCTGG

Cytotoxicity Assay

Cells were seeded in 48 well plates (Corning Inc., Corning, NY) using DMEM/F12 media with 10% FBS and 1% penicillin and streptomycin. The plates were then incubated at 37˚C, 5% CO_2. After 24 hours, the media was changed for serum free DMEM/F12 media. The plates were incubated at 37˚C and 5% CO_2 for another 24 hours, after which the media was replaced with fresh new serum free DMEM/F12 media and an appropriate concentration of H_2O_2 (0.5 - 1.0 μM) was added. For adenovirus-transduced cells, application of H_2O_2 was done 48 hours after adenovirus transduction. 18 hours after the application of H_2O_2, the supernatant from the wells were collected and transferred to a 96 well plate (Corning Inc., Corning, NY) for the cytotoxicity assay. Lactate dehydrogenase (LDH) release from the cytoplasm of damaged cells was measured using the CytoTox 96 Non-Radioactive Cytotoxicity Assay kit (Promega Corp, Madison, WI) according to the manufacturer's directions. Results of the assay were quantified using the

ELISA plate reader (Dynatech Medica, Guernsey, UK) to measure the absorbance at 490nm.

Choroidal Sprouting Assay

The choroidal sprouting assay was conducted according to a previously published method [58] with some modifications. Eyes were collected from 3 week-old C57Bl/6J mice (The Jackson Laboratory, Bar Harbor, ME) and immediately placed in cold phosphate buffered saline (PBS, Sigma-Aldrich) containing 1% penicillin and streptomycin. Under sterile conditions, the anterior portion of each eye was dissected out and the retina was removed leaving the choroid/sclera complex intact. The posterior eyecups were cut radially, transferred into 5cm dishes, and maintained inside a large drop (50µl) of serum free DMEM media (Lonza) supplemented with 1% penicillin and streptomycin (Lonza). After all the tissues were collected, the media was replaced with either 50µl of Ad-GFP (conc: 1 x 10^5 pfu/µl) or 50µl of Ad-PGC1B (conc: 1 x 10^5 pfu/µl) diluted in DMEM. The samples were incubated for 6 hours at 37˚C and 10% CO_2 for efficient adenoviral infection. After the incubation period, the media was removed and the samples were quickly washed 2-3 times using EGM-2 media with 5% FBS and 1% penicillin and streptomycin. Using a 1mm punch biopsy (Integra Miltex, York, PA), 4-5 samples were punched out from the peripheral region of the choroid/sclera complex. Each explant was added to a sterile 12mm coverslip coated with 30µl of growth factor-reduced matrigel (Corning, Corning, NY). The explants were incubated at 37˚C and 5% CO_2 for 10 minutes to allow the matrigel to solidify. Afterwards, the coverslips containing the

embedded explants were placed into a 24 well plate with 0.5ml of EGM-2 5% FBS, 1% penicillin and streptomycin added. Every 48 hours, the media was replaced with fresh new EGM-2 media with 5% FBS, 1% penicillin and streptomycin and the explants were imaged using an inverted microscope. The sprouting area for each explant was quantified using the ImageJ software (National Institutes of Health, version 1.51h).

Immunohistochemistry

Forty-eight hours following adenoviral infection, the choroidal explants were fixed using 4% paraformaldehyde (PFA, Electron Microscopy Sciences, Hatfield, PA) and incubated at room temperature for 20 minutes. The fixative was removed and the samples were washed 3 times for 20 min with PBS before incubation for 1 hour in a blocking buffer that consisted of 1% bovine serum albumin (BSA) and 0.1% Tween (Sigma-Aldrich) in PBS. The filamentous actin (F-actin) of the RPE was stained using a 1:300 dilution of Alexa Flour 594 phalloidin (Invitrogen, Carlsbad, CA) followed by a wash with PBS. The cell nuclei were stained using a 1:1000 dilution of 4', 6-diamidino-2-phenylindole (DAPI) followed by another wash with PBS. Images were taken at 10X and 40X magnification using the Axioskop (Carl Zeiss Microscopy, Thornwood, NY).

Conditioned Media Preparation

ARPE-19 cells were seeded using DMEM/F12 with 10% FBS and 1% penicillin and streptomycin in a 6 well plate at a density of 30,000 cells/cm^2. The following day, one of the wells was trypsinized for cell counting using the counter coulter (Beckman

Coulter, Fullerton, CA). The media is then removed and replaced with serum free DMEM/F12 along with either Ad-GFP, Ad-PGC1A, or Ad-PGC1B at a MOI of 100. Eighteen hours after the adenovirus infection, the media was replaced with DMEM/F12 media supplemented with 1% FBS and 1% penicillin and streptomycin and the cells were left to recover for 24 hours. After this period, the media was replaced with 2ml of DMEM/F12 with 1% FBS for 48 hours conditioning. After the conditioning period, the media was collected from each well, centrifuged at 1500 rpm for 5 minutes to remove large cellular debris and stored at -80˚C for later use.

Cell Proliferation Assay

RF/6A cells were seeded in three 96 well plates at a density of 50,000 cells/well using MEM media with 10% FBS and 1% penicillin and streptomycin. The following day, the cells were starved overnight using DMEM/F12 media with 1% FBS. Afterwards, the media was removed and the cells were treated with conditioned media from either Ad-GFP, Ad-PGC1A, Ad-PGC1B, or untreated ARPE-19 cells. The MTT Vybrant kit was used according to the manufacturer's instructions in order to perform the cell proliferation assay. The absorbance was measured at 540nm using the ELISA plate reader (Dynatech Medica, Guernsey, UK).

Cell Migration Assay

Cell migration was evaluated using the standard cell scratch assay.[59] RF/6A cells were seeded at confluency into 12 well plates. The following day, the growth media was

removed and cells were starved in DMEM/F12 media with 1% FBS and 1% penicillin and streptomycin overnight. Then the media was removed and a 200µl pipette tip was used to make a vertical scratch in the center of each well. Each well was washed twice with PBS to remove all floating cells and appropriate experimental conditioned media (CM) was added. The plates were incubated at 37˚C and 5% CO_2 and images of the wells were taken at 0, 6, and 24 hours after the CM was applied to the wells using the EVOS microscope at 4X magnification. The area of the scratch was quantified using ImageJ software (National Institutes of Health, version 1.51h).

Tube Formation Assay

Fifty microliters of basal membrane extract (BME) was added to each well of a 96 well plate. Then, the plate was incubated at 37˚C for 1 hour to allow the BME to solidify. Meanwhile, confluent RF/6A cells that were serum starved overnight using MEM media were trypsinized, counted, and re-suspended in DMEM/F12 media with 1% FBS and 1% penicillin and streptomycin at a concentration of 1,000,000 cells/ml. Fifty microliters of the cell suspension (50,000 cells) were added to each well and the plate was then incubated at 37˚C and 5% CO_2 for at least 1 hour to allow the cells to adhere to the BME. Once the cells adhered to the BME, the media was removed and replaced with 50 µl of CM. The plate was incubated at 37˚C and 5% CO_2 for 10 hours. Images of tube formation were taken at 4X and 10X magnification using the EVOS microscope.

Statistical Analysis

Statistical analysis of data was performed using GraphPad Prism 5 software (GraphPad Software Inc., La Jolla, CA). Values are presented as mean ± SEM unless otherwise stated. The student's t-test was used for analysis of experiments comparing two conditions whereas the one-way ANOVA with the Dunnett's multiple comparison post test was used for analysis of experiments using three or more conditions. Statistical significance is denoted by the following: * $P < 0.05$, ** $P < 0.01$, *** $P < 0.001$, **** $P < 0.0001$.

RESULTS

Gene Analysis of Adenovirus-Transduced ARPE-19 Cells

Total RNA was collected from ARPE-19 cells that were transduced at a MOI of 300 with either Ad-GFP or Ad-PGC1B. qPCR was performed to determine how the gene expression of transcription factors regulating certain antioxidant and metabolic proteins were affected by overexpression of PGC1B in ARPE-19 cells compared to control cells (cells overexpressing ad-GFP). Quantification of qPCR data (Figure 4) demonstrated that PGC1B overexpression significantly induced the expression of the *PPARA* (p=0.0021), *ESRRA* (p=0.0005), *SOD2* (p=0.0003), and *TXN2* (p=0.0076) genes compared to the control cells. The analysis also showed that PGC1B repressed the expression of the *PPARGC1A* (p=0.0033), *NFE2L2* (p=0.0023), and *FOXO3* (p=0.0058) genes. There was no statistically significant difference between ARPE-19 cells overexpressing the *PPARAGC1B* gene and control ARPE-19 cells overexpressing the GFP gene in the expression of *PPARAGC1B*, *CAT*, *HMOX1*, and *NRF1* genes. This shows that contrary to PGC1A,[54] PGC1B represses the expression of essential antioxidant transcription factors and enzymes in the RPE which could result in increased oxidative stress within the cells.

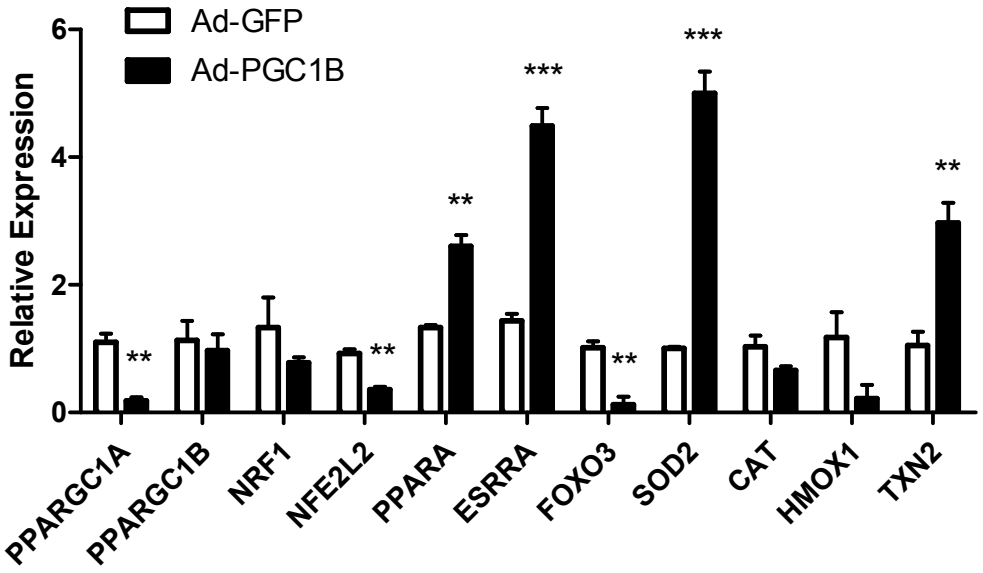

Figure 4: PGC1B overexpression modulates key transcription factor genes. PGC1B overexpression in ARPE-19 cells leads to the repression of PPARGC1A (PGC1A) and transcription factors important for antioxidant enzyme expression such as *FOXO3* and *NFE2L2* while inducing the expression of transcription factors important for oxidative metabolism such as *PPARA* and *ESRRA* (n=3). Data analyzed using Student's T test.

Overexpression of PGC1B Leads to Increased Cytotoxicity in RPE Cells

The capability of PGC1B to induce RPE cell death under basal and pro-oxidative conditions was evaluated by measuring lactate dehydrogenase release (a marker of necrosis and late apoptosis) from ARPE-19 cells treated with or without hydrogen peroxide (H_2O_2). Hydrogen peroxide is a reactive oxygen species that is produced during mitochondrial respiration and phagocytosis of photoreceptor outer segments.[60] Parental ARPE-19 cells were treated with 0, 250, 500, or 1000μM of H_2O_2 for 14 or 18 hours. Cell death increased in these cells in a time and dose dependent manner (Figure 5A). Then, ARPE-19 cells infected at MOI 100 with either Ad-GFP or Ad-PGC1B were

treated with 0 or 500μM H_2O_2 for 18 hours. It was demonstrated that ARPE-19 cells overexpressing PGC1B had a significantly higher percentage of cell death with and without H_2O_2 treatment than the control ARPE-19 cells treated with Ad-GFP (Figure 5B). This shows that induction of PGC1B expression in the RPE places it at increased risk of dysfunction and cell death.

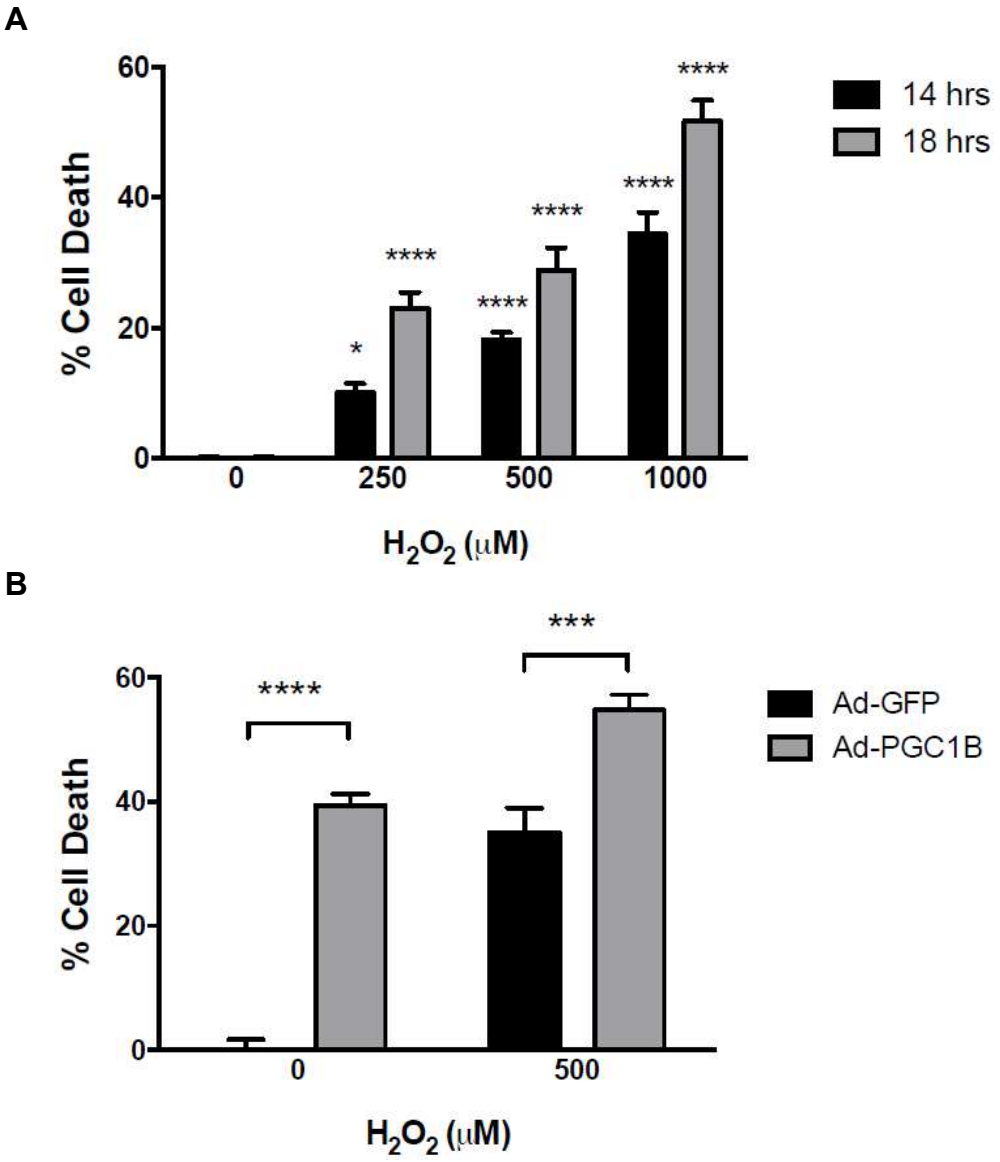

Figure 5: Overexpression of PGC1B Leads to Increased Cell Death. (A) The cytotoxic effect of H_2O_2 was tested on parental ARPE-19 cells in a time and dose dependent manner (n=5). Data analyzed using Two-way ANOVA. (B) ARPE-19 cells infected with Ad-PGC1B showed increased cell death compared to control ARPE-19 cells infected with Ad-GFP with and without H_2O_2 treatment (n=5). Data analyzed using Two-way ANOVA.

Choroidal Sprouting Assay Shows Evidence that Overexpression of PGC1B Leads to Angiogenesis

The pro-angiogenic effect of PGC1B was evaluated by performing a choroidal sprouting assay. This new *ex vivo* angiogenesis model allowed us to evaluate microvascular growth in an organotypic system.[57] In order to characterize the effect of PGC1B expression in RPE on choroidal microvascular outgrowth, we first needed to develop a method for overexpressing PGC1B in choroidal explants as native healthy RPE cells do not express this gene.[54] Using our previously characterized adenoviral method for infection of cell culture, we investigated the ability of Ad-GFP and Ad-PGC1B to efficiently infect RPE cells in live ocular posterior cups. Eyes were collected from young adult wild type albino mice (3 week old Swiss Webster). The inside of the posterior eye cups (RPE) were exposed to 25 x 10^5 pfu of Ad-GFP or Ad-PGC1B for 6 hours and maintained in culture for up to 48 hours to allow for the expression of the transduced genes. We used a combination of direct GFP detection and immunohistochemistry for the cytoskeleton marker F-actin to confirm high infection of both Ad-GFP and Ad-PGC1B of RPE cells in the posterior cups (Figure 6A). Total RNA was collected from the entire eyecup 48 hours following adenoviral infection and qPCR was performed to evaluate the gene expression levels of eGFP, *Ppargc1a* (PGC1A), and *Ppargc1b* (PGC1B). Analysis showed a robust increase in the gene expression of PGC1B in Ad-PGC1B treated eyecups when compared to the control Ad-GFP infected tissue ($p<0.05$). Importantly, we also confirmed that PGC1B overexpression does not alter basal expression of PGC1A

(Figure 6B). These results demonstrated that PGC1B was successfully overexpressed in the RPE cells of murine posterior eyecups that were adenovirus-transduced.

Once PGC1B gain of function in live ocular tissue was established, we performed a choroidal explant sprouting assay using 3 week old C57Bl/6J mice (Figure 7A). Quantification of the sprouting areas showed that after 6 days in culture, the explants with RPE overexpressing PGC1B had a larger sprouting area than explants with RPE overexpressing GFP ($p=0.0127$). After 8 days, the sprouting area for both conditions continued to increase. While the sprouting area of explants with RPE overexpressing PGC1B was still larger than the sprouting area of explants with RPE overexpressing GFP, the difference was not statistically significant ($p=0.5187$) (Figure 7B). The choroid sprouting assay demonstrated that overexpression of PGC1B in RPE increases choroidal angiogenesis.

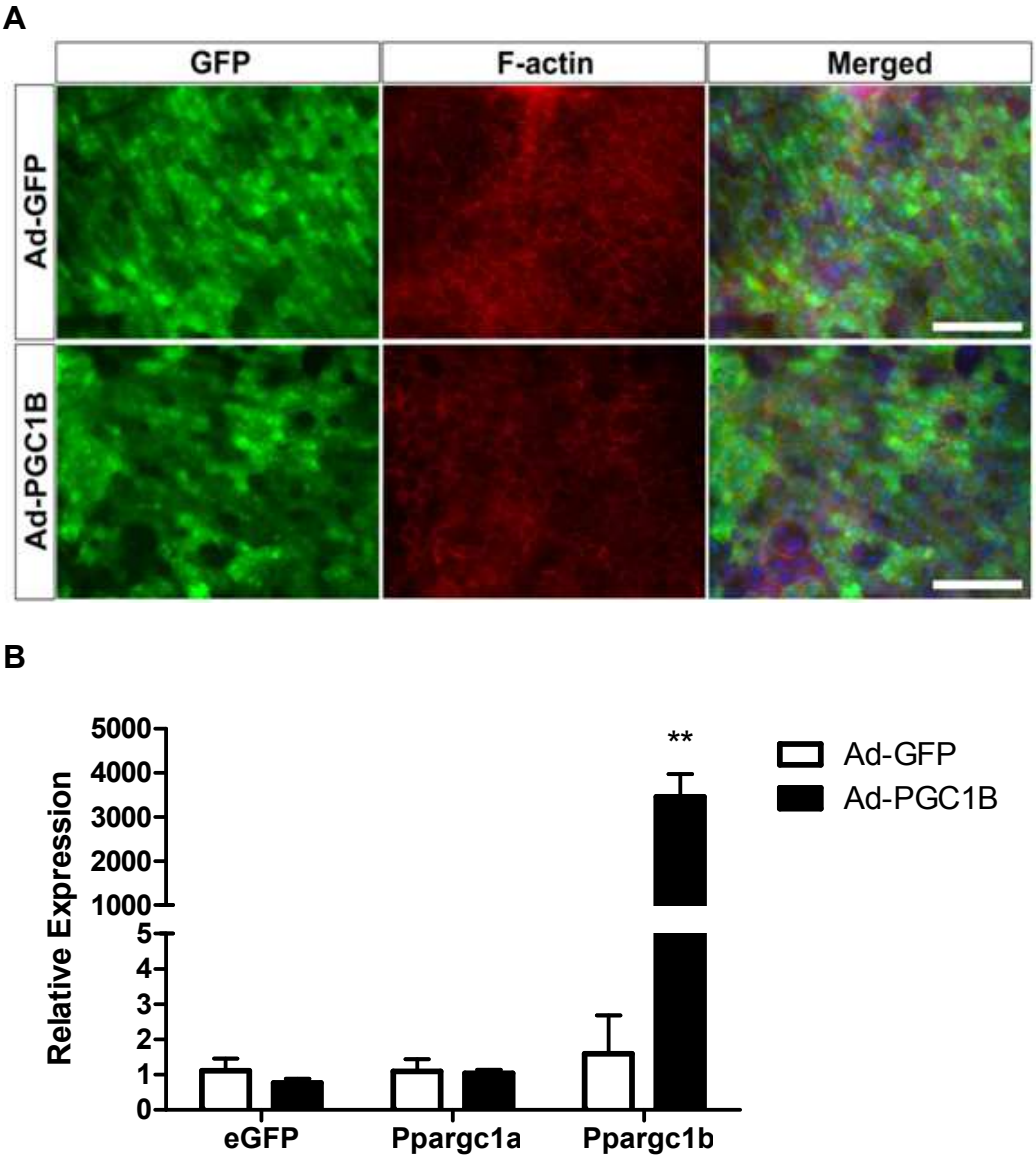

Figure 6: Efficiency of PGC1B overexpression in mouse choroidal explants. (A) Immunostaining of Swiss Webster mice explants confirms that the RPE identified by their characteristic cuboidal shape (see F-actin staining) have been efficiently infected with either Ad-GFP or Ad-PGC1B. (B) Gene expression analysis of choroidal explants 48 hours after infection with either Ad-GFP or Ad-PGC1B (n=3). Data analyzed using Student's T test.

A

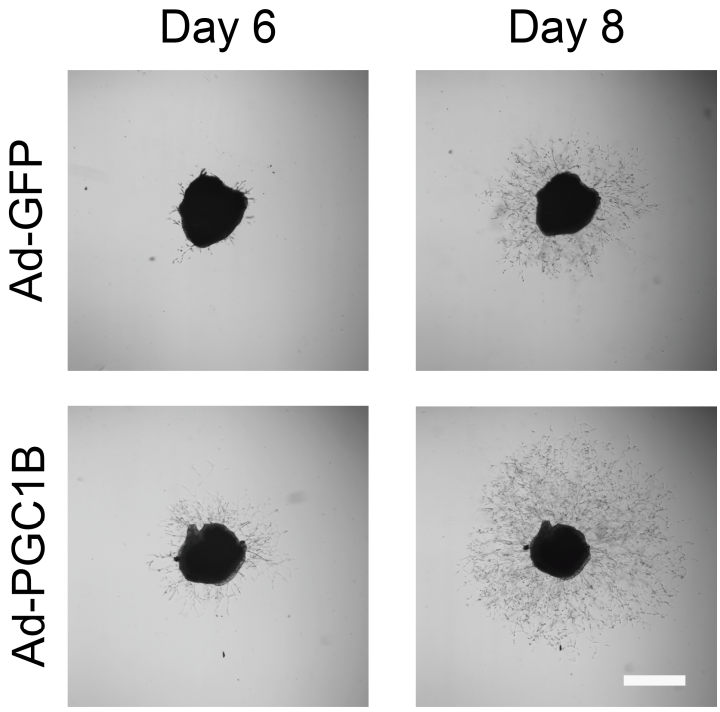

B

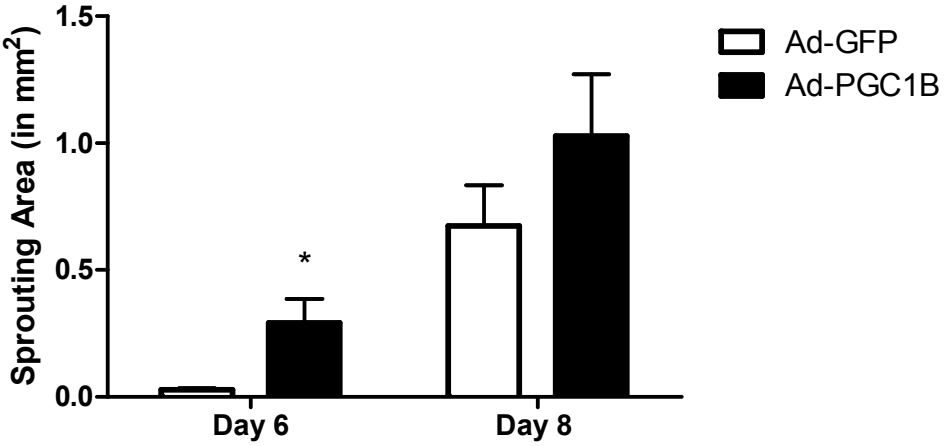

Figure 7: *Ex Vivo* Choroid Sprouting Assay. (A) Photographs of choroidal explants and their sprouting area. Scale bar = 100μm. (B) Quantification of sprouting area shows that explants infected with Ad-PGC1B had an increased sprouting area compared to the control explants infected with Ad-GFP (n=9). Data analyzed using Student's T test.

MTT Assay Shows That PGC1B Overexpression Increases RF/6A Cell Proliferation

Angiogenesis occurs via a series of complex cellular processes mainly associated with the proliferation and migration of endothelial cells. To better understand which of these phenomena was activated during PGC1B-induced choroidal sprouting, we first evaluated the effect of PGC1B overexpression on the ability of RPE to promote endothelial cell (EC) proliferation using the rhesus monkey chorioretinal cell line (RF/6A) as an EC model. RF/6A cells were exposed to CM from untreated or infected ARPE-19 with Ad-GFP or Ad-PGC1B and their proliferation was evaluated using the MTT assay. It was observed that proliferation of RF/6A cells was increased 24 ($p<0.001$) and 48 hours ($p<0.0001$) after treatment with CM from ARPE-19 cells infected with PGC1B as compared to control ARPE-19 cells infected with Ad-GFP (Figure 8). This shows further evidence that overexpression of PGC1B in RPE cells can lead to the secretion of factors that can promote angiogenesis in the choroid of the eye.

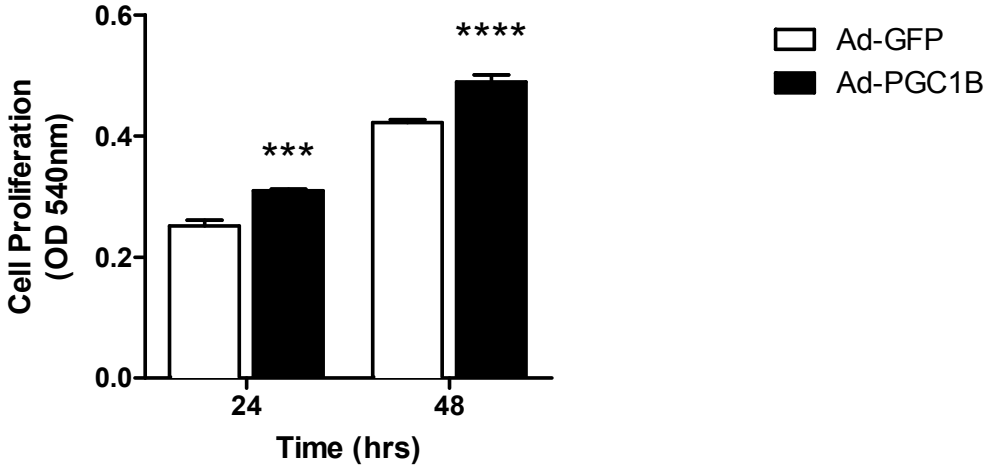

Figure 8: Effect of ARPE-19 conditioned media on RF/6A proliferation. The increased optical density (OD) suggests that RF/6A proliferation was significantly increased over the control after 24 and 48 hours of treatment with conditioned media from ARPE-19 cells infected with Ad-PGC1B (n=3). Data analyzed using Two-way ANOVA followed by Sidak's multiple comparison test.

Cell Migration and Tube Formation Assays Show No Evidence of Angiogenesis as a Result of PGC1B Induction

In order to further investigate the pro-angiogenic effect of PGC1B, we performed a cell migration assay by making a vertical scratch through a monolayer of RF/6A cells and evaluating the area of scratch closure after 6 or 24 hours. In one experiment, RF/6A cells were treated with basal unconditioned media (DMEM/F12 1% FBS), full unconditioned media (EGM-2 5% FBS), or conditioned media from uninfected ARPE-19 cells. After 24 hours, cell migration was highest in RF/6A cells treated with full unconditioned media as the scratch closure was approximately 80%. There was a significant increase in cell migration for RF/6A cells that were treated with unconditioned

full media (EGM-2 5% FBS) compared to RF/6A cells that were treated with unconditioned basal media (DMEM/F12 1% FBS) ($p<0.0001$). There was also a significant increase in cell migration for RF/6A cells treated with full unconditioned media compared to RF/6A cells treated with conditioned media from uninfected ARPE-19 cells ($p<0.0001$). There was no significant difference in cell migration between RF/6A cells treated with unconditioned basal media and RF/6A cells treated with basal conditioned media from uninfected ARPE-19 cells (Figure 9A).

In another experiment, conditioned media from ARPE-19 cells was mixed at a 1:1 ratio with the full unconditioned media. After 6 hours of incubation at 37°C, there was no significant difference in cell migration between RF/6A cells treated with conditioned media from uninfected ARPE-19 cells, RF/6A cells treated with conditioned media from Ad-GFP infected ARPE-19 cells, or RF/6A cells treated with conditioned media from Ad-PGC1B infected ARPE-19 cells. After 24 hours, the percent scratch closure for all three conditions was approximately 80% which was similar to the scratch closure for RF/6A cells treated with full unconditioned media after 24 hours. There was no significant difference in cell migration among the three conditions (Figure 9B).

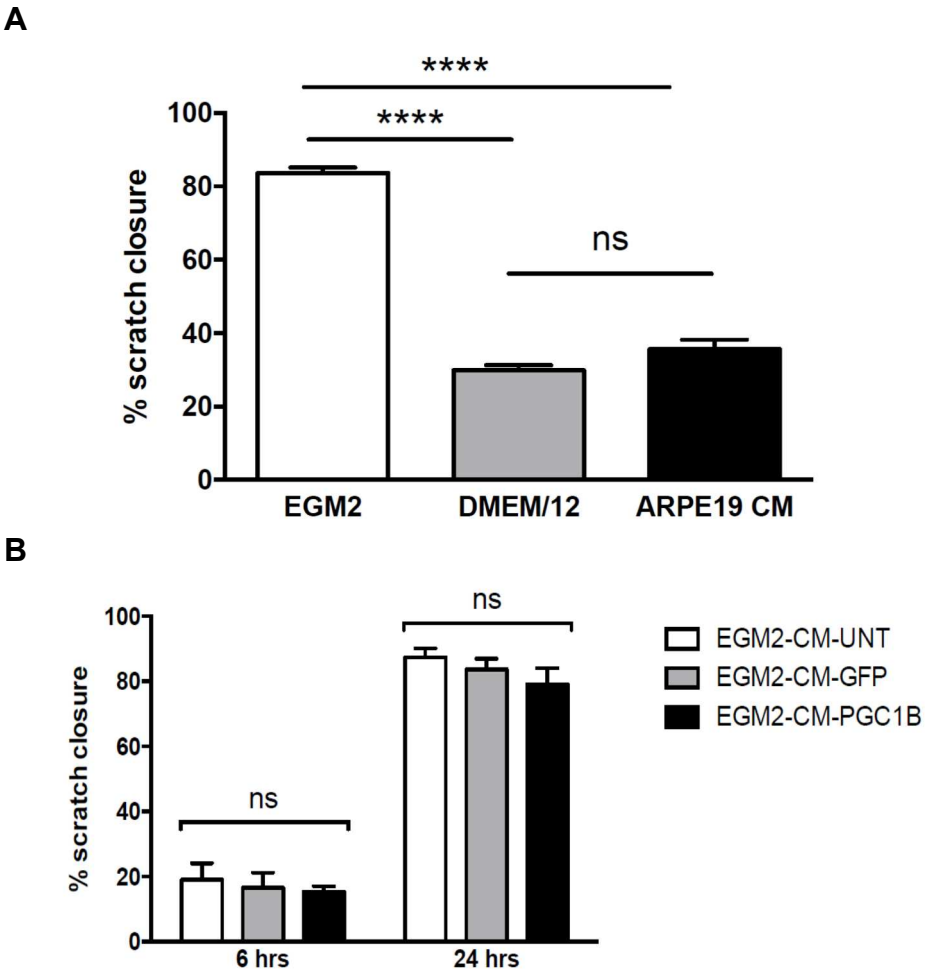

Figure 9: Evaluating migratory activity of RF/6A cells. (A) RF/6A migration activity evaluated by percent scratch closure after treatment for 24 hours with full unconditioned media (EGM2), basal unconditioned media (DMEM/F12), and basal conditioned media (ARPE-19 CM) (n=3). Data analyzed by One-way ANOVA followed by Tukey's multiple comparisons test. (B) RF/6A migration evaluated by scratch closure after treatment with conditioned media mixed 1:1 with full unconditioned media. Data analyzed by Two-way ANOVA followed by Tukey's multiple comparisons test.

Conditions allowing for RF6A tube formation on BME were first tested. Two different media (MEM with 10% FBS and EGM-2 5% FBS) and two different cell

densities (20,000 and 50,000 cells) were evaluated. Formation of tube-like structures following 6 hours of incubation at 37°C was only observed when 50,000 cells were plated and exposed to EGM-2 media (Figure 10). As with the scratch assay, we elected to test ARPE-19 derived CM mixed at a 1:1 ratio with EGM-2 5% FBS in order to evaluate the pro-angiogenic effect of PGC1B expression. Evaluation of CM from uninfected cells show significantly increased tube formation as shown by larger covered area ($p=0.0045$), tube length ($p=0.0068$), and branching points ($p=0.0097$) compared to non-conditioned media (Table 3). However, similar comparative analysis of CM from Ad-GFP and Ad-PGC1B infected cells showed no significant change in the extent or characteristics of the tubes formed (Table 3), suggesting that contrary to our previous results using choroidal explants, PGC1B gain of function in ARPE-19 does not promote angiogenesis, at least under the conditions tested here.

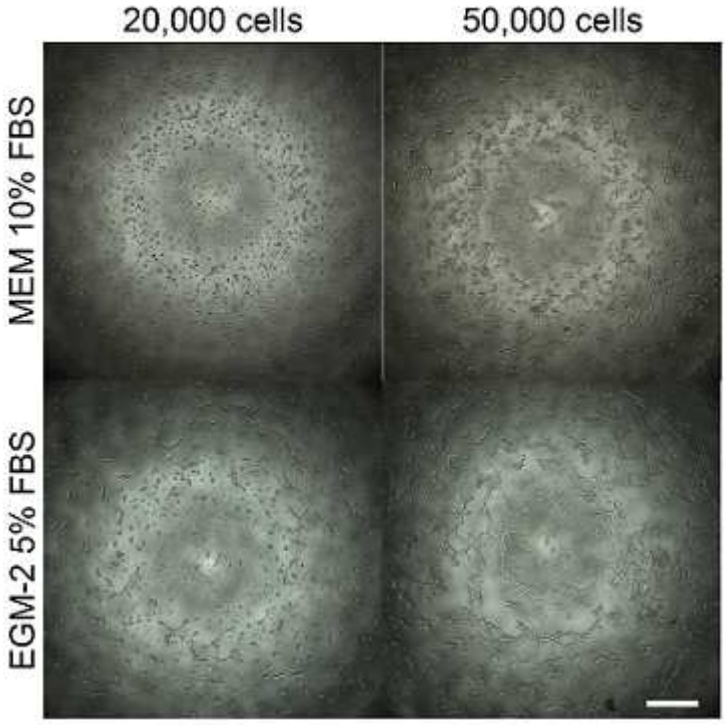

Figure 10: Tube Formation Assay. Qualitative analysis shows that tube-like structures formed when cells were plated at 50,000 cells using EGM-2 media with 5% FBS. Scale bar = 500µm.

Table 3: Tube Characteristics. Quantification of tube formation parameters for ARPE-19 CM shows significantly increased tube formation for uninfected cells as compared to non-conditioned media (BM). However, comparison between Ad-GFP and Ad-PGC1B infected ARPE-19 cells show no significant change (n=4). Data analyzed using Student's T test.

Tube Characteristics						
	BM	Uninfected	P value	Ad-GFP	Ad-PGC1B	P value
Covered Area (%)	15.45 ± 2.33	30.03 ± 6.18	**0.0045	25.62 ± 4.28	23.43 ± 4.12	0.4865
Tube Length (px)	12187 ± 1240	20270 ± 3814	**0.0068	17102 ± 2357	14819 ± 2280	0.2132
Branching Points	8.5 ± 3	56.25 ± 25.46	**0.0097	38.25 ± 15.65	24.75 ± 11.79	0.2173
Number of Loops	0 ± 0	11.75 ± 11.59	0.0888	3.75 ± 2.87	1.25 ± 1.5	0.1737

DISCUSSION

In this study, we show that induction of PGC1B increases RPE metabolic activity by inducing the expression of the *PPARA* and *ESRRA* genes. These genes encode for transcription factors that regulate metabolic activities in the RPE cell such as lipid and amino acid metabolism.[61] As the metabolism of the RPE cell is increased, the activity of the electron transport chain is increased at the same time, leading to superoxide accumulation. Previous work in our lab has shown that PGC1A gain of function is accompanied by both an increase in *PPARA* and *ESRRA* expression (that will induce oxidative metabolism) and in two critical antioxidant transcriptional regulators, *FOXO3 and NFE2L2*.[54] Here we show that, contrary to PGC1A, PGC1B gain of function greatly represses *FOXO3 and NFE2L2* expression which could alter the level of antioxidant enzymes in RPE and induce ROS accumulation. Indeed we showed that while *SOD2* gene expression is significantly increased when PGC1B is overexpressed, the *CAT* gene is not (Figure 2). SOD2 is responsible for converting the ROS produced as byproducts of the electron transport chain into hydrogen peroxide and diatomic oxygen.[62] Catalase is needed to convert hydrogen peroxide into water and diatomic oxygen.[63] Without increased CAT expression, accumulation of hydrogen peroxide within the RPE cell would increase basal and H_2O_2-dependent cell death, which was confirmed in this study (Figure 3).

In addition to promoting oxidative damage and cell death in RPE, clinical evidence suggests that increase in PGC1B may promote choroidal neovascularization.

We were able to confirm this hypothesis by adenovirally expressing PGC1B (normally repressed) in the RPE of entire mouse posterior eye cups that were subsequently used in a choroidal sprouting assay. However, subsequent analysis of the different cellular processes involved in microvascular sprouting, i.e. proliferation and migration of choroidal endothelial cells exposed to conditioned media of native or transduced ARPE-19, led to contradictory results. RF/6A migration and tube formation was poor or nonexistent when 100% conditioned media from infected ARPE-19 cells was used. It was only when the conditioned media was mixed at a 1:1 ratio with a highly enriched media used for endothelial cell expansion that robust cell migration and tube formation was observed. But this demonstrates that cell migration and tube formation occurred only because a more pro-angiogenic medium was being used and not because of the conditioned media alone. Since it was shown in the preliminary data that PGC1B suppresses the activity of anti-angiogenic factors, it must be questioned whether the RF/6A is the correct endothelial cell model to evaluate PGC1B's angiogenic potential. According to the ATCC, the RF/6A cell line was spontaneously transformed and passaged over 450 times [64] which means that it may have lost some of its original cellular characteristics. Alternatives that can be used include iPSC-derived choroid endothelial cells [65] and human retinal endothelial cells. Another alternative are primary human choroidal endothelial cells, but concerns have been raised about access to fresh donor samples, high variability in the samples obtained, and loss of cell characteristics after isolation and expansion in vitro.[66,67]

Also, the results of the MTT assay have to be called into question. The MTT assay uses metabolic activity, specifically the activity of succinate dehydrogenase in the mitochondria, as a measure of the number of living cells present.[68] Increased activity of the enzyme theoretically should mean that there are more cells present. Since overexpression of PGC1B has been shown in this study to increase metabolic activity (Figure 2), it is possible that there was an increase in metabolic activity of the RF/6A cells but not a corresponding increase in cell number. However, it is important to note that PGC1A overexpression, which also leads to increased mitochondrial biogenesis and function, was not associated with increased MTT reduction. Nevertheless, these results must be confirmed using other measures of cell proliferative activity such as bromodeoxyuridine (BrdU) incorporation, flow cytometry analysis of DNA content and/or ki-67 expression.

It is interesting to note that this study has shown that PGC1B overexpression in ARPE-19 cells did not significantly affect endogenous PGC1B gene expression levels but led to the suppression of PGC1A. Iacovelli et al have shown that maturation of RPE cells in vitro leads to the induction of PGC1A expression while PGC1B expression is repressed.[54] The same study has shown that induction of PGC1A promotes the expression of transcription factors such as FOXO3 and NFE2L2 that regulate antioxidant enzymes that protect the RPE cell from cell dysfunction and death due to oxidative stress. An important question that would need to be answered through further investigation is whether the suppression of *FOXO3* and *NFE2L2* is caused directly by PGC1B expression or by the suppression of PGC1A.

Since this study has confirmed that PGC1B has detrimental effects on the RPE cell, this provides opportunities for further research to be conducted to develop novel therapeutic strategies in order to block the unfavorable effects of PGC1B to ameliorate some of the symptoms of AMD. While no loss of function studies were performed in this study, it is imperative to evaluate how loss of function of PGC1B would affect the RPE cell and determine whether silencing PGC1B expression would be beneficial in combating the harmful effects of AMD. Another strategy is to potentially target signaling factors upstream of PGC1B to prevent its upregulation, although further investigation would be needed to fully comprehend the mechanism of PGC1B induction.

REFERENCES

1. Cheung LK, Eaton A. Age-related macular degeneration. *Pharmacotherapy*. 2013; 33(8): 838-55.

2. Rein DB, Wittenborn JS, Zhang X, et al. Forecasting age-related macular degeneration through the year 2050: the potential impact of new treatments. *Archives of ophthalmology*. 2009; 127(4): 533-40.

3. Rudnicka AR, Jarrar Z, Wormald R, Cook DG, Fletcher A, Owen CG. Age and gender variations in age-related macular degeneration prevalence in populations of European ancestry: a meta-analysis. *Ophthalmology*. 2012; 119(3): 571-80.

4. Smith W, Assink J, Klein R, et al. Risk factors for age-related macular degeneration: Pooled findings from three continents. *Ophthalmology*. 2001; 108(4): 697-704.

5. Thornton J, Edwards R, Mitchell P, Harrison RA, Buchan I, Kelly SP. Smoking and age-related macular degeneration: a review of association. *Eye*. 2005; 19(9): 935-44.

6. Chakravarthy U, Wong TY, Fletcher A, et al. Clinical risk factors for age-related macular degeneration: a systematic review and meta-analysis. *BMC Ophthalmology*. 2010; 10:31.

7. Fisher DE, Klein BE, Wong TY, et al. Incidence of Age-Related Macular Degeneration in a Multi-Ethnic United States Population: The Multi-Ethnic Study of Atherosclerosis. *Ophthalmology*. 2016; 123(6): 1297-308.

8. Klein RJ, Zeiss C, Chew EY, et al. Complement factor H polymorphism in age-related macular degeneration. *Science*. 2005; 308(5720): 385-9.

9. Donoso LA, Vrabec T, Kuivaniemi H. The role of complement Factor H in age-related macular degeneration: a review. *Survey of Ophthalmology*. 2010; 55(3): 227-46.

10. Gold B, Merriam JE, Zernant J, et al. Variation in factor B (BF) and complement component 2 (C2) genes is associated with age-related macular degeneration. *Nature Genetics*. 2006; 38(4): 458-62.

11. Fritsche LG, Chen W, Schu M, et al. Seven new loci associated with age-related macular degeneration. *Nature Genetics*. 2013; 45(4): 433-9, 439e1-2.

12. Kanda A, Chen W, Othman M, et al. A variant of mitochondrial protein LOC387715/ARMS2, not HTRA1, is strongly associated with age-related macular degeneration. *Proceedings of the National Academy of Sciences of the United States of America*. 2007; 104(41): 16227-32.

13. Jager RD, Mieler WF, Miller JW. Age-related macular degeneration. *New England Journal of Medicine*. 2008; 358(24): 2606-17.

14. Klein R, Myers CE, Lee KE, et al. Small Drusen and Age-Related Macular Degeneration: The Beaver Dam Eye Study. *Journal of Clinical Medicine*. 2015; 4(3): 424-40.

15. Bird AC, Bressler NM, Bressler SB, et al. An international classification and grading system for age-related maculopathy and age-related macular degeneration. The International ARM Epidemiological Study Group. *Survey of Ophthalmology*. 1995; 39(5): 367-74.

16. Klein R, Klein BE, Linton KL. Prevalence of age-related maculopathy. The Beaver Dam Eye Study. *Ophthalmology*. 1992; 99(6): 933-43.

17. Age-Related Eye Disease Study Research Group. The Age-Related Eye Disease Study system for classifying age-related macular degeneration from stereoscopic color fundus photographs: the Age-Related Eye Disease Study Report Number 6. *American Journal of Ophthalmology*. 2001; 132(5): 668-81.

18. Cheung CM, Wong TY. Is age-related macular degeneration a manifestation of systemic disease? New prospects for early intervention and treatment. *Journal of Internal Medicine*. 2014; 276(2): 140-53.

19. Age-Related Eye Disease Study Research Group. A randomized, placebo-controlled, clinical trial of high-dose supplementation with vitamins C and E, beta

carotene, and zinc for age-related macular degeneration and vision loss: AREDS report no. 8. *Archives of Ophthalmology*. 2001; 119(10): 1417-36.

20. Evans JR, Lawrenson JG. A review of the evidence for dietary interventions in preventing or slowing the progression of age-related macular degeneration. *Ophthalmic & physiological optics: the journal of the British College of Ophthalmic Opticians*. 2014; 34(4): 390-6.

21. Ferrara N, Damico L, Shams N, Lowman H, Kim R. Development of ranibizumab, an anti-vascular endothelial growth factor antigen binding fragment, as therapy for neovascular age-related macular degeneration. *Retina*. 2006; 26(8): 859-70.

22. Tufail A, Patel PJ, Egan C, et al. Bevacizumab for neovascular age related macular degeneration (ABC Trial): multicentre randomised double masked study. *British Medical Journal*. 2010; 340:c2459.

23. Singerman LJ, Masonson H, Patel M, et al. Pegaptanib sodium for neovascular age-related macular degeneration: third-year safety results of the VEGF Inhibition Study in Ocular Neovascularisation (VISION) trial. *The British Journal of Ophthalmology*. 2008; 92(12): 1606-11.

24. Dixon JA, Oliver SC, Olson JL, Mandava N. VEGF Trap-Eye for the treatment of neovascular age-related macular degeneration. *Expert Opinion on Investigational Drugs*. 2009; 18(10): 1573-80.

25. Strauss O. The retinal pigment epithelium in visual function. *Physiological Reviews*. 2005; 85(3): 845-81.

26. Balaban RS, Nemoto S, Finkel T. Mitochondria, oxidants, and aging. *Cell*. 2005; 120(4): 483-95.

27. Nguyen T, Nioi P, Pickett CB. The Nrf2-antioxidant response element signaling pathway and its activation by oxidative stress. *Journal of Biological Chemistry*. 2009; 284(20): 13291–5.

28. Beatty S, Koh H, Phil M, Henson D, Boulton M. The role of oxidative stress in the pathogenesis of age related macular degeneration. *Survey of Ophthalmology*. 2000; 45(2): 115–34.

29. Cai J, Nelson KC, Wu M, Sternberg P, Jones DP. Oxidative damage and protection of the RPE. *Progress in retinal and eye research*. 2000; 19(2): 205–21.

30. Imamura Y, Noda S, Hashizume K, et al. Drusen, choroidal neovascularization, and retinal pigment epithelium dysfunction in SOD1-deficient mice: a model of age-related macular degeneration. *Proceedings of the National Academy of Sciences of the United States of America*. 2006; 103(30): 11282–7.

31. Justilien V, Pang J-J, Renganathan K, et al. SOD2 knockdown mouse model of early AMD. *Investigative Ophthalmology & Visual Science*. 2007; 48(10): 4407–20.

32. Zhao Z, Chen Y, Wang J, et al. Age-related retinopathy in NRF2-deficient mice. *PLoS ONE*. 2011; 6(4): e19456.

33. Zhao C, Yasumura D, Li X, et al. mTOR-mediated dedifferentiation of the retinal pigment epithelium initiates photoreceptor degeneration in mice. *Journal of Clinical Medicine*. 2011; 121(1): 369–83.

34. Mao H, Seo S-J, Biswal MR, et al. Mitochondrial oxidative stress in the retinal pigment epithelium leads to localized retinal degeneration. *Investigative Ophthalmology & Visual Science*. 2014; 55(7): 4613–27.

35. Karunadharma PP, Nordgaard CL, Olsen TW, Ferrington DA. Mitochondrial DNA damage as a potential mechanism for age-related macular degeneration. *Investigative Ophthalmology & Visual Science*. 2010; 51(11): 5470–9.

36. Arnouk H, Lee H, Zhang R, Chung H, Hunt RC, Jahng WJ. Early biosignature of oxidative stress in the retinal pigment epithelium. J Proteomics. 2011; 74(2): 254–61.

37. Sachdeva MM, Cano M, Handa JT. Nrf2 signaling is impaired in the aging RPE given an oxidative insult. *Experimental eye research*. 2014; 119:111–4.

38. Karunadharma PP, Nordgaard CL, Olsen TW, Ferrington DA. Mitochondrial DNA damage as a potential mechanism for age-related macular degeneration. *Investigative Ophthalmology & Visual Science*. 2010; 51(11): 5470–9.

39. Kaarniranta K, Sinha D, Blasiak J, et al. Autophagy and heterophagy dysregulation leads to retinal pigment epithelium dysfunction and development of age-related macular degeneration. *Autophagy*. 2013; 9(7): 973–84

40. Tseng WA, Thein T, Kinnunen K, et al. NLRP3 Inflammasome Activation in Retinal Pigment Epithelial Cells by Lysosomal Destabilization: Implications for Age-Related Macular Degeneration. *Investigative Ophthalmology & Visual Science*. 2013; 54(1): 110–20.

41. Kauppinen A, Niskanen H, Suuronen T, Kinnunen K, Salminen A, Kaarniranta K. Oxidative stress activates NLRP3 inflammasomes in ARPE-19 cells--implications for age-related macular degeneration (AMD). *Immunology Letters*. 2012; 147(1-2): 29–33.

42. Tarallo V, Hirano Y, Gelfand BD, et al. DICER1 loss and Alu RNA induce age-related macular degeneration via the NLRP3 inflammasome and MyD88. *Cell*. 2012; 149(4): 847–59.

43. Altman BJ, Rathmell JC. Metabolic stress in autophagy and cell death pathways. *Cold Spring Harbor Perspectives in Biology*. 2012; 4(9): a008763.

44. Mootha VK, Handschin C, Arlow D, et al. Erralpha and Gabpa/b specify PGC-1alpha-dependent oxidative phosphorylation gene expression that is altered in diabetic muscle. *Proceedings of the National Academy of Sciences of the United States of America*. 2004; 101(17): 6570-5

45. Wu Z, Puigserver P, Andersson U, et al. Mechanisms controlling mitochondrial biogenesis and respiration through the thermogenic coactivator PGC-1. *Cell*. 1999; 98(1): 115-24.

46. Patten IS, Arany Z. PGC-1 coactivators in the cardiovascular system. *Trends in endocrinology and metabolism*. 2012; 23(2): 90–7.

47. Handschin C, Spiegelman BM. Peroxisome proliferator-activated receptor gamma coactivator 1 coactivators, energy homeostasis, and metabolism. *Endocrine Reviews*. 2006; 27(7): 728–35.

48. Lin J, Handschin C, Spiegelman BM. Metabolic control through the PGC-1 family of transcription coactivators. *Cell Metabolism*. 2005; 1(6): 361–70.

49. St-Pierre J, Drori S, Uldry M, et al. Suppression of reactive oxygen species and neurodegeneration by the PGC-1 transcriptional coactivators. *Cell*. 2006; 127(2): 397–408.

50. Lin J, Wu H, Tarr PT, et al. Transcriptional co-activator PGC-1 alpha drives the formation of slow-twitch muscle fibres. *Nature*. 2002; 418(6899): 797–801.

51. Yoon JC, Puigserver P, Chen G, et al. Control of hepatic gluconeogenesis through the transcriptional coactivator PGC-1. *Nature*. 2001; 413(6852): 131–8.

52. Saint-Geniez M, Jiang A, Abend S, et al. PGC-1α regulates normal and pathological angiogenesis in the retina. *American Journal of Pathology*. 2013; 182(1): 255–65.

53. Egger A, Samardzija M, Sothilingam V, et al. PGC-1α determines light damage susceptibility of the murine retina. *PLoS ONE*. 2012; 7(2): e31272.

54. Iacovelli J, Rowe GC, Khadka A, et al. PGC-1α Induces Human RPE Oxidative Metabolism and Antioxidant Capacity. *Investigative Ophthalmology & Visual Science*. 2016; 57(3): 1038-51.

55. Handa JT, Cano M, Wang L, Datta S, Liu T. Lipids, oxidized lipids, oxidation-specific epitopes, and Age related Macular Degeneration. *Biochimica et biophysica acta*. 2017; 1862(4): 430-440. Epub 2016 Jul 30.

56. Gnanaguru G, Choi AR, Amarnani D, D'Amore PA. Oxidized Lipoprotein Uptake Through the CD36 Receptor Activates the NLRP3 Inflammasome in Human Retinal Pigment Epithelial Cells. *Investigative Ophthalmology & Visual Science*. 2016; 57(11): 4704–12.

57. Lehman JJ, Barger PM, Kovacs A, Saffitz JE, Medeiros DM, Kelly DP. Peroxisome proliferator-activated receptor gamma coactivator-1 promotes cardiac mitochondrial biogenesis. *Journal of Clinical Investigation*. 2000; 106(7): 847-56.

58. Shao Z, Friedlander M, Hurst CG, et al. Choroid sprouting assay: an ex vivo model of microvascular angiogenesis. *PLoS One*. 2013; 8(7): e69552.

59. Liang CC, Park AY, Guan JL. In vitro scratch assay: a convenient and inexpensive method for analysis of cell migration in vitro. *Nature Protocols*. 2007; 2(2): 329-33.

60. Miceli MV, Liles MR, Newsome DA. Evaluation of oxidative processes in human pigment epithelial cells associated with retinal outer segment phagocytosis. *Experimental Cell Research*. 1994; 214(1): 242-9.

61. Contreras AV, Torres N, Tovar AR. PPAR-α as a key nutritional and environmental sensor for metabolic adaptation. *Advances in Nutrition*. 2013; 4(4): 439-52.

62. McCord JM, Fridovich I. Superoxide dismutase. An enzymic function for erythrocuprein (hemocuprein). *Journal of Biological Chemistry*. 1969; 244(22): 6049-55.

63. Putnam CD, Arvai AS, Bourne Y, Tainer JA. Active and inhibited human catalase structures: ligand and NADPH binding and catalytic mechanism. *Journal of Molecular Biology*. 2000; 296(1): 295-309.

64. RF/6A. ATCC. https://www.atcc.org/en/Products/Cells_and_Microorganisms/By_Tissue/Retina/CRL-1780.aspx#characteristics. Accessed March 11, 2017.

65. Songstad AE, Wiley LA, Duong K, et al. Generating iPSC-Derived Choroidal Endothelial Cells to Study Age-Related Macular Degeneration. *Investigative Ophthalmology & Visual Science.* 2015; 56(13): 8258–67.

66. Lacorre D-A, Baekkevold ES, Garrido I, et al. Plasticity of endothelial cells: rapid dedifferentiation of freshly isolated high endothelial venule endothelial cells outside the lymphoid tissue microenvironment. *Blood.* 2004; 103(11): 4164–72.

67. Aird WC. Phenotypic Heterogeneity of the Endothelium: I. Structure, Function, and Mechanisms. *Circulation Research.* 2007; 100(2): 158–73.

68. Wang P, Henning SM, Heber D. Limitations of MTT and MTS-based assays for measurement of antiproliferative activity of green tea polyphenols. *PLoS One*. 2010; 5(4): e10202.

CURRICULUM VITAE